

Letter

Augmentation of humoral and cellular immune responses after third-dose SARS-CoV-2 vaccination and viral neutralization in myeloma patients

Adolfo Aleman,^{1,2,3,15} Oliver Van Oekelen,^{1,2,3,15} Bhaskar Upadhyaya,^{2,3} Katherine Beach,^{4,5} Ariel Kogan Zajdman,^{2,3} Hala Alshammary,^{4,5} Kseniya Serebryakova,^{2,3} Sarita Agte,^{2,3} Katerina Kappes,^{2,3} Charles R. Gleason,⁴ Komal Srivastava,^{4,5} PVI/MM/Seronet Study Group, Steve Almo,⁶ Carlos Cordon-Cardo,^{5,7,8} Florian Krammer,^{4,5} Miriam Merad,^{2,3,8,9,10} Sundar Jagannath,^{2,3} Ania Wajnberg,^{11,12} Viviana Simon,^{4,5,13,14,*} and Samir Parekh^{2,3,8,10,*}

¹Graduate School of Biomedical Sciences, Icahn School of Medicine at Mount Sinai, New York, NY, USA

²Department of Medicine, Hematology, and Medical Oncology, Icahn School of Medicine at Mount Sinai, New York, NY, USA

³Tisch Cancer Institute, Icahn School of Medicine at Mount Sinai, New York, NY, USA

⁴Department of Microbiology, Icahn School of Medicine at Mount Sinai, New York, NY, USA

⁵Department of Pathology, Molecular and Cell-Based Medicine, Icahn School of Medicine at Mount Sinai, New York, NY, USA

⁶Department of Biochemistry, Albert Einstein College of Medicine, New York, NY, USA

⁷Department of Genetics and Genomic Sciences, Icahn School of Medicine at Mount Sinai, NY, USA

⁸Department of Oncological Sciences, Icahn School of Medicine at Mount Sinai, New York, NY, USA

⁹Human Immune Monitoring Center, Icahn School of Medicine at Mount Sinai, New York, NY, USA

¹⁰Precision Immunology Institute, Icahn School of Medicine at Mount Sinai, New York, NY, USA

¹¹Department of Internal Medicine, Icahn School of Medicine at Mount Sinai, New York, NY, USA

¹²Department of Geriatrics and Palliative Medicine, Icahn School of Medicine at Mount Sinai, NY, USA

¹³Division of Infectious Disease, Department of Medicine, Icahn School of Medicine at Mount Sinai, New York, NY, USA

¹⁴Global Health and Emerging Pathogen Institute, Icahn School of Medicine at Mount Sinai, New York, NY, USA

¹⁵These authors contributed equally

*Correspondence: viviana.simon@mssm.edu (V.S.), samir.parekh@mssm.edu (S.P.)

<https://doi.org/10.1016/j.ccell.2022.03.013>

Despite the efficacy of COVID-19 vaccines in healthy individuals, multiple myeloma (MM) patients are immunocompromised and mount suboptimal humoral and cellular responses after two doses of mRNA vaccine (Addeo et al., 2021; Aleman et al., 2021; Van Oekelen et al., 2021). A broader observation of limited vaccine responses in cancer patients, particularly those with hematologic malignancies (Thakkar et al., 2021), has led to the implementation of additional (i.e., third-dose) vaccine administration as a way to increase protection for patients with immune suppression. A third dose of BNT162b2 (Pfizer-BioNTech) COVID-19 vaccine has shown to be effective in preventing severe COVID-19 caused by the SARS-CoV-2 B.1.617.2 (Delta) variant in the general population (Bar-On et al., 2021; Barda et al., 2021). Furthermore, third-dose administration of either the BNT162b2 (Pfizer-BioNTech) or mRNA-1273 (Moderna) COVID-19 vaccine was associated with augmented immune responses in a diverse cohort of cancer patients (Shapiro et al., 2022). However, the real-world effectiveness of additional dosing in myeloma patients and viral neutralization have not been reported. Additionally, the impact of the currently

dominant SARS-CoV-2 B.1.1.529 (Omicron) variant on efficacy of the third dose is largely unknown in patients with hematologic malignancies (Zeng et al., 2022).

We studied the humoral and cellular immune response to COVID-19 vaccination longitudinally in a real-world cohort of 476 MM patients and compared it with data of age-matched vaccinated health-care workers. Of the full cohort, 354 patients (74%) had anti-SARS-CoV-2 spike (S) IgG levels collected at least 6 months after two doses of mRNA vaccine, and 261 (55%) had anti-S IgG measured at least 1 week after the third dose administration. Summarized demographic characteristics of the cohort are shown in Table S1. The study cohort was predominantly male (57%), with a median age of 67 years (range 38–96 years). Forty patients (8%) were included with a diagnosis of smoldering MM. Patients included had received a median of two lines of treatment (range 0–16) at the time of initial vaccination. Of note, documented COVID-19 infection occurred in 124 patients (26%) at any time during the pandemic.

The serologic effect of the third dose is illustrated in Figure S1A. Patients were split by COVID-19 infection status (i.e.,

whether they developed COVID-19 before or at any time after the initial vaccination) to separate the effect of natural infection. Anti-S IgG level increased significantly after administration of the third dose, both in patients with COVID-19 (median 110 AU/mL after dose 2 to 381 AU/mL after dose 3, $p < 0.001$) and in patients without COVID-19 (median 27 AU/mL after dose 2 to 161 AU/mL after dose 3, $p < 0.001$). To better characterize the benefit of the third vaccine dose, we specifically looked at the 241 MM patients for whom anti-S IgG levels were available at time points both before and after the third dose (i.e., paired samples). Sixty-eight patients (28%) were seronegative (i.e., they had no detectable anti-S IgG) at the last time point collected prior to the third dose (median 183 days post dose 2, range 15–336 days). Of these, 60/68 (88%) developed detectable anti-S IgG after dose 3 (median 0 AU/mL after dose 2 to 45.5 AU/mL after dose 3) (Figure S1B, sero-conversion). Of 173 patients who had measurable anti-S IgG after two doses, anti-S IgG increased in 158 patients (91%) after dose 3 (median 43 AU/mL after dose 2 to 300 AU/mL after dose 3) (Figure S1B, sero-elevation). Although the third dose provided a robust



boost to serological status, MM patients that were in both the sero-conversion and the sero-elevation group had significantly lower serological levels than age-matched healthy donors (HDs) after three doses (Figure S1B, $p < 0.001$).

Initial two-dose vaccination was associated with a significantly weaker responses among MM patients treated with anti-CD38 monoclonal antibodies (mAb) or BCMA-targeted therapy (Aleman et al., 2021; Van Oekelen et al., 2021). In patients who did not develop COVID-19, the third dose resulted in significant increases of anti-S IgG across all treatment groups (Figure S1C), including in patients receiving an anti-CD38 mAb ($p < 0.001$) or a BCMA-targeted therapy (chimeric antigen receptor (CAR) T cell therapy, bispecific antibody therapy, or antibody-drug conjugate) ($p < 0.01$), although the level of anti-S IgG after dose 3 in patients on anti-CD38 mAb remained significantly lower in comparison to MM patients that did not receive active treatment (median 121 versus 312 AU/mL, $p < 0.01$).

In a subset of 31 patients, we analyzed cellular and neutralizing responses. We characterized the cellular responses in a subset of 14 sero-conversion MM patients, 17 sero-elevation MM patients, and 13 seropositive HDs, before and after third mRNA vaccination, using high-dimensional flow cytometry. The third vaccination dose resulted in a significant increase in spike-reactive B cells in MM patients in both the sero-elevation and sero-conversion groups ($p < 0.05$, Figure S1D). The presence of spike-reactive memory B cells also strongly correlated with the magnitude of detectable anti-S IgG antibody titers ($r = 0.6$, $p < 0.001$). Spike-specific T cell responses were measured by stimulating peripheral blood mononuclear cells (PBMC) with a pool of spike peptides (15-mer sequences with an 11 amino acid overlap spanning the entire spike protein) and quantifying cytokine-producing cells in CD4⁺ T cells expressing CD154 and CD69. Total cytokine-expressing CD4⁺ T cells were estimated by aggregating activated CD4⁺ T cells producing GM-CSF, IFN- γ , IL-2, IL-4, IL-17, and TNF- α . In sero-conversion and sero-elevation MM patients, we observed a significant increase in spike-specific CD4⁺ T cell-mediated cytokine responses after the third dose ($p < 0.05$, Figure S1E). In HD, however, B and T cell responses were not

significantly augmented after the administration of the third vaccination.

To better characterize the protection against infection, we compared the effect of a third-dose vaccination on the neutralizing capacity to WA1, the wild-type virus, across MM patients and HD (Figure S1F). The sero-conversion group of MM patients was most vulnerable, with no subjects having detectable neutralization capacity prior to third dose. Only half (7/13, 54%) of the MM patients in the sero-elevation group had neutralizing titers, compared to 80% (8/10) of HD prior to third vaccination. Although the third vaccination dose increased neutralizing capacity against WA1, only 40% (2/5) of sero-conversion MM patients had neutralizing titers, which was strikingly lower than the 92% (12/13) of sero-elevation MM patients and 100% of HD ($n = 10/10$) achieving detectable neutralizing titers (Figure S1G).

An important outstanding question remains as to whether the mRNA vaccine-induced immune response offers adequate protection against SARS-CoV-2 variants. For the Omicron variant specifically, evasion of (humoral) immunity from vaccination or infection with earlier variants has been reported due to the accumulation of mutations in the spike protein gene (McCallum et al., 2022; Zeng et al., 2022). This is especially relevant for patients with pre-existing immune deficiency (e.g., hematologic malignancy), who could be at higher risk of severe infection. In our cohort, we observed a peak with 40 cases of COVID-19 diagnosed after December 1, 2021 (Figure S1H), coinciding with the Omicron variant becoming dominant locally. Seventeen of these patients had already received a third dose. In these patients, anti-S IgG levels collected within 90 days prior to developing COVID-19 in the Omicron-dominant period were highly variable (median 51 AU/mL; range 0–2,511 AU/mL) and were non-significantly ($p = 0.3$) lower when compared to anti-S IgG levels collected in the same time period for subjects after three doses of vaccine who did not develop COVID-19 (median 201 AU/mL; range 0–4,078 AU/mL) (Figure S1I).

We compared the effect of a third-dose vaccination on the neutralizing activity against the Omicron variant using sera from MM patients and HD collected before and after the third vaccine dose

(Figure S1J). Neutralizing titers against the Omicron variant were detectable after third-dose vaccination in all HDs (100%, 10/10), in contrast to only 54% (7/13) of sero-elevation MM patients and none of the sero-conversion MM patients (0%, 0/5, Figure S1K). Omicron-neutralizing antibody titers correlated with anti-S IgG antibody levels ($r = 0.68$, $p < 0.001$, Figure S1L) as well as the magnitude of cellular spike-reactive B cells ($r = 0.55$, $p < 0.001$, Figure S1M).

In our data, a high fraction of MM patients (28%) had undetectable anti-S IgG prior to dose 3, suggesting that the initial humoral response to two vaccine doses is not only suboptimal (Terpos et al., 2021; Van Oekelen et al., 2021) but also decreases and, in some cases, disappears over time. We here show that the third dose induces sero-conversion in more than 80% of the MM patients with undetectable anti-S IgG. However, this population may remain vulnerable, as shown by the lack of neutralization capacity of ancestral (e.g., WA1) as well as emerging viral variants of concern (e.g., Omicron). Our findings indicate that a third mRNA vaccine dose significantly augments cellular and humoral immune responses against SARS-CoV-2, including the antigenically distinct Omicron variant, in MM patients. Therefore, patients with MM should be encouraged to receive the third dose when eligible. Sera from less than half of the MM patients in our study were able to neutralize the Omicron variant, although it should be noted that prior to the third dose virtually all MM patients had an undetectable neutralizing titer. These findings underscore the need for continued monitoring of immune responses and further research around measures such as additional vaccine doses or passive immunization for individual MM patients that may remain vulnerable after third-dose vaccination, especially as COVID-19 restrictions are being lifted worldwide and new waves of viral variants are emerging.

SUPPLEMENTAL INFORMATION

Supplemental information can be found online at <https://doi.org/10.1016/j.ccell.2022.03.013>.

ACKNOWLEDGMENTS

We thank participants for their generosity and willingness to participate in longitudinal COVID-19

research studies. None of this work would be possible without their contributions. We acknowledge the clinical and research staff at the Center of Excellence for Multiple Myeloma at Mount Sinai. S.P. is supported by National Cancer Institute (NCI) R01 CA244899, CA252222 and receives research funding from Amgen, Celgene/BMS, and Karyopharm. This work was partially funded by the NIAID Collaborative Influenza Vaccine Innovation Centers (CIVIC) contract 75N93019C00051, NIAID Center of Excellence for Influenza Research and Surveillance (CEIRS, contracts HHSN272201400008C and HHSN272201400006C), and NIAID grants U01AI141990 and U01AI150747; by the generous support of the JPB Foundation and the Open Philanthropy Project (research grant 2020-215611 [5384]); and by anonymous donors. This effort was supported by the Serological Sciences Network (SeroNet) in part with federal funds from the National Cancer Institute, National Institutes of Health, under contract 75N91019D00024, task order 75N91021F00001. This work was supported by The Price Family Foundation (SCA), the Wollowick Family Foundation Chair in Multiple Sclerosis and Immunology (SCA), the Einstein-Rockefeller-CUNY Center for AIDS Research (P30AI124414), and the Einstein Macromolecular Therapeutics Development Facility supported by the Albert Einstein Cancer Center (P30CA013330). The content of this publication does not necessarily reflect the views or policies of the Department of Health and Human Services, nor does mention of trade names, commercial products, or organizations imply endorsement by the U.S. Government. We acknowledge support of the Center of Excellence for Multiple Myeloma Philanthropy.

AUTHOR CONTRIBUTIONS

V.S., A.W., S.P., and PVI study group provided conceptualization, methodology, analysis, and resources for this work. A.A., O.V.O., K.K., K.B., K. Serebryakova, S.A., C.R.G., K. Srivastava, and PVI were involved in organizational aspects of the clinical studies, patient recruitment, data collection, and analysis. A.A., O.V.O., S.A., C.R.G., C.C.-C., and F.K. were involved in design, data collection, analysis, visualization, and interpretation of serological data. A.A., B.U., K.T., and A.K.Z. were involved in design, execution, analysis, visualization, and interpretation of T and B and T cell assays. S.J., A.W., S.P., V.S., and MM Clinical Group were involved in different aspects of patient care. A.A., O.V.O., B.U., M.M., S.J., A.W., V.S., and S.P. provided interpretation of the data and conceptualization of the first manuscript draft.

A.A., O.V.O., B.U., A.W., V.S., and S.P. contributed to the writing of the first manuscript draft. H.A., V.S., C.R.G., K. Srivastava, K.B., and PVI study group were involved in neutralization assays and serological quantification. The Almo lab made recombinant spike protein used in spike-reactive B cell identification. All coauthors provided critical edits to the initial manuscript draft and approved the final version.

DECLARATION OF INTERESTS

The Icahn School of Medicine at Mount Sinai has filed patent applications relating to SARS-CoV-2 serological assays and NDV-based SARS-CoV-2 vaccines which list Florian Krammer as co-inventor. Viviana Simon and Carlos Cardon-Cordo are listed on the serological assay patent application as co-inventors. Mount Sinai has spun out a company, Kantaro, to market serological tests for SARS-CoV-2. Ajai Chari reports grants and personal fees from Janssen, Bristol Myers Squibb (Celgene), Amgen, Seattle Genetics, and Millennium Pharmaceuticals/Takeda and personal fees from Karyopharm, Sanofi, Oncopeptides, Antengene, Glaxo Smith Kline, Secura Bio, Shattuck Labs, Genentech, and Abbvie. Florian Krammer reports grants and personal fees from Pfizer and personal fees from Seqirus and Avimex. The Krammer laboratory is collaborating with Pfizer on animal models of SARS-CoV-2. Sundar Jagannath reports consulting fees for Bristol Myers Squibb (Celgene), Janssen, Karyopharm Therapeutics, Merck, Sanofi, and Takeda Pharmaceuticals. Samir Parikh reports consulting fees from Foundation Medicine and research funding from Bristol Myers Squibb (Celgene), Karyopharm, and Amgen. The other authors reported no relevant conflicts of interest.

REFERENCES

Addeo, A., Shah, P.K., Bordry, N., Hudson, R.D., Albracht, B., Di Marco, M., Kaklamani, V., Dietrich, P.-Y., Taylor, B.S., Simand, P.-F., et al. (2021). Immunogenicity of SARS-CoV-2 messenger RNA vaccines in patients with cancer. *Cancer Cell* 39, 1091–1098.e2.

Aleman, A., Upadhyaya, B., Tuballes, K., Kappes, K., Gleason, C.R., Beach, K., Agte, S., Srivastava, K., Van Oekelen, O., Barcessat, V., et al.; PVI/Seronet Study Group (2021). Variable cellular responses to SARS-CoV-2 in fully vaccinated patients with multiple myeloma. *Cancer Cell* 39, 1442–1444.

Bar-On, Y.M., Goldberg, Y., Mandel, M., Bodenheimer, O., Freedman, L., Kalkstein, N., Mizrahi, B., Alroy-Preis, S., Ash, N., Milo, R., and Huppert, A. (2021). Protection of BNT162b2 vaccine booster against Covid-19 in Israel. *N. Engl. J. Med.* 385, 1393–1400.

Barda, N., Dagan, N., Cohen, C., Hernán, M.A., Lipsitch, M., Kohane, I.S., Reis, B.Y., and Balicer, R.D. (2021). Effectiveness of a third dose of the BNT162b2 mRNA COVID-19 vaccine for preventing severe outcomes in Israel: an observational study. *Lancet* 398, 2093–2100.

McCallum, M., Czudnochowski, N., Rosen, L.E., Zepeda, S.K., Bowen, J.E., Walls, A.C., Hauser, K., Joshi, A., Stewart, C., Dillen, J.R., et al. (2022). Structural basis of SARS-CoV-2 Omicron immune evasion and receptor engagement. *Science* 375, 864–868.

Shapiro, L.C., Thakkar, A., Campbell, S.T., Forest, S.K., Pradhan, K., Gonzalez-Lugo, J.D., Quinn, R., Bhagat, T.D., Choudhary, G.S., McCort, M., et al. (2022). Efficacy of booster doses in augmenting waning immune responses to COVID-19 vaccine in patients with cancer. *Cancer Cell* 40, 3–5.

Terpos, E., Gavriatopoulou, M., Ntanasis-Stathopoulos, I., Briasoulis, A., Gumeni, S., Malandrakis, P., Fotiou, D., Papanagnou, E.-D., Migkou, M., Theodorakakou, F., et al. (2021). The neutralizing antibody response post COVID-19 vaccination in patients with myeloma is highly dependent on the type of anti-myeloma treatment. *Blood Cancer J.* 11, 138.

Thakkar, A., Gonzalez-Lugo, J.D., Goradia, N., Gali, R., Shapiro, L.C., Pradhan, K., Rahman, S., Kim, S.Y., Ko, B., Sica, R.A., et al. (2021). Seroconversion rates following COVID-19 vaccination among patients with cancer. *Cancer Cell* 39, 1081–1090.e2.

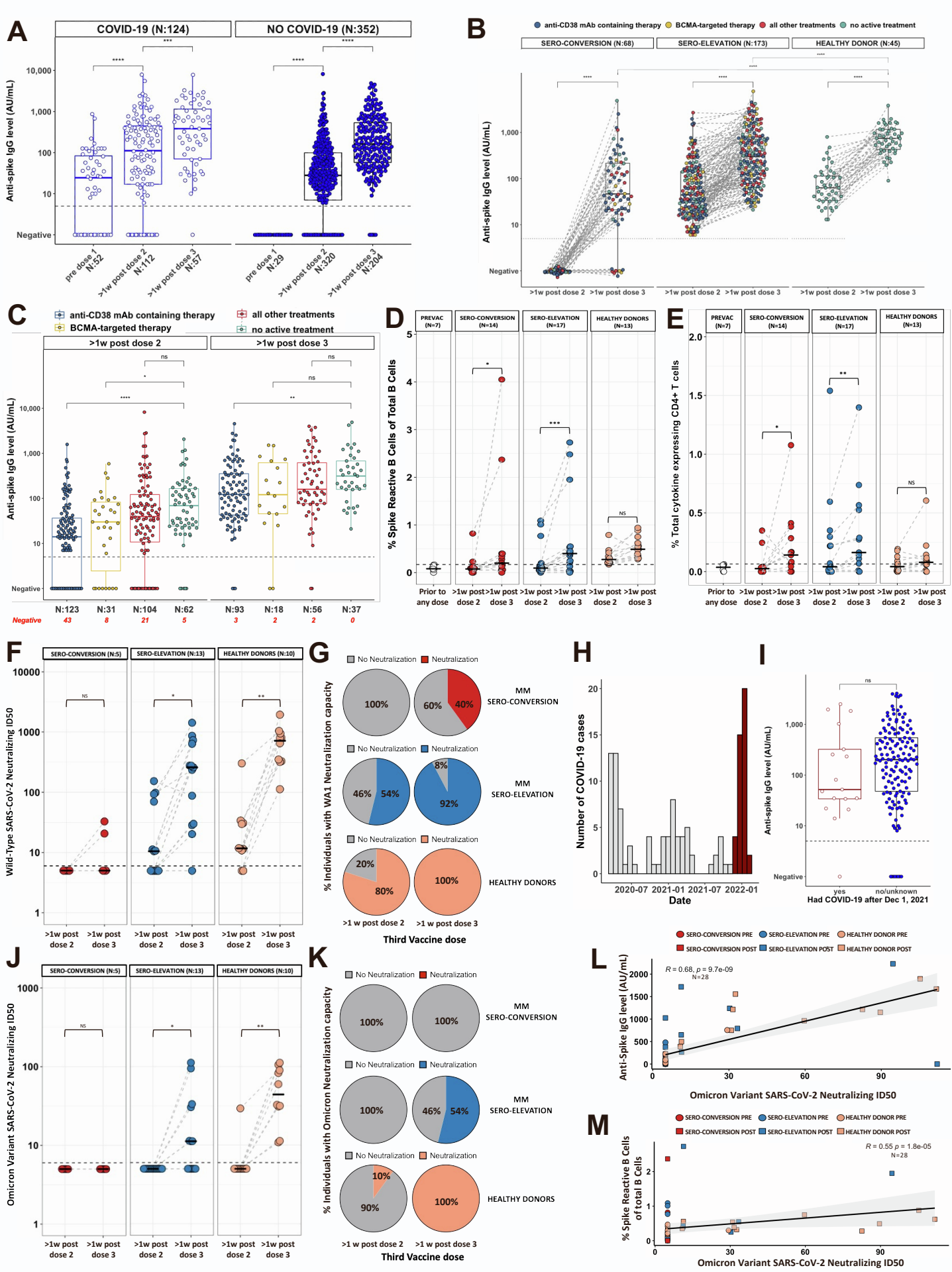
Van Oekelen, O., Gleason, C.R., Agte, S., Srivastava, K., Beach, K.F., Aleman, A., Kappes, K., Mouhieddine, T.H., Wang, B., Chari, A., et al.; PVI/Seronet team (2021). Highly variable SARS-CoV-2 spike antibody responses to two doses of COVID-19 RNA vaccination in patients with multiple myeloma. *Cancer Cell* 39, 1028–1030.

Zeng, C., Evans, J.P., Chakravarthy, K., Qu, P., Reisinger, S., Song, N.J., Rubinstein, M.P., Shields, P.G., Li, Z., and Liu, S.L. (2022). COVID-19 mRNA booster vaccines elicit strong protection against SARS-CoV-2 Omicron variant in patients with cancer. *Cancer Cell* 40, 117–119.

Supplemental information

**Augmentation of humoral and cellular immune
responses after third-dose SARS-CoV-2 vaccination
and viral neutralization in myeloma patients**

Adolfo Aleman, Oliver Van Oekelen, Bhaskar Upadhyaya, Katherine Beach, Ariel Kogan Zajdman, Hala Alshammary, Kseniya Serebryakova, Sarita Agte, Katerina Kappes, Charles R. Gleason, Komal Srivastava, PVI/MM/Seronet Study Group, Steve Almo, Carlos Cordon-Cardo, Florian Krammer, Miriam Merad, Sundar Jagannath, Ania Wajnberg, Viviana Simon, and Samir Parekh



1 **Supplemental Figure S1. Humoral and cellular responses to SARS-CoV-2**
2 **vaccination in patients with multiple myeloma. (A)** Time course of anti-SARS-CoV-2
3 spike (S) IgG antibody levels in multiple myeloma (MM) patients split by COVID-19
4 infection status. Antibody concentrations measured in artificial units per mL (AU/mL) and
5 are depicted on a log-10 scale. The horizontal dotted line indicates the lower limit of
6 detection (5 AU/mL). **(B)** Effect of SARS-CoV-2 third vaccination on anti-S IgG antibody
7 levels in MM patients and age-matched healthy donors (HD). Dots are colored to indicate
8 treatment regimen at the time of vaccination. Antibody concentrations measured in
9 artificial units per mL (AU/mL) and are depicted on a log-10 scale. The horizontal dotted
10 line indicates the lower limit of detection (5 AU/mL). **(C)** Anti-S IgG antibody levels at least
11 7 days after receiving two doses of SARS-CoV-2 mRNA vaccine and at least 7 days after
12 receiving three doses of SARS-CoV-2 mRNA vaccine in MM patients split according to
13 major treatment groups. None of the depicted patients in this panel developed COVID-19
14 at any point during the pandemic. Antibody concentrations measured in artificial units per
15 mL (AU/mL) and are depicted on a log-10 scale. The horizontal dotted line indicates the
16 lower limit of detection (5 AU/mL). **(D)** Frequencies of SARS-CoV-2 spike-reactive B cells
17 in different cohorts within the CD19⁺ gate. The horizontal dotted line indicates the highest
18 observed frequency of total spike-reactive B cells in the unvaccinated HD control cohort.
19 The bold horizontal line indicates the median for each group. **(E)** SARS-CoV-2 specific
20 CD4⁺ T cell responses in MM patients and HD. Total cytokine-expressing CD4⁺ T cells
21 were estimated by aggregating activated CD4⁺ T cells producing GM-CSF, IFN- γ , IL-2,
22 IL-4, IL-17, and TNF- α . Frequencies were calculated by subtracting water control
23 frequencies from the CD4⁺ T cell response for each subject. The horizontal dotted line

24 indicates highest observed frequency of total cytokine response in the unvaccinated HD
25 control cohort. The bold horizontal line indicates the median for each group. **(F)**
26 Neutralizing antibody ID50 to WA1 wild-type SARS-CoV-2 strain for MM subject groups
27 and HD. The bold horizontal line indicates the median for each group. **(G)** Quantification
28 of MM patients and HD that achieve neutralization to the WA1, wildtype strain >1 week
29 post dose 2 and >1 week post dose 3. **(H)** Histogram representing COVID-19 infection
30 cases in MM patients at Mount Sinai Hospital between March 2020 and January 2021.
31 Dark red overlay indicates cases during the period when the Omicron variant was
32 dominant in New York. **(I)** Anti-S IgG antibody levels in MM patients that contracted
33 COVID-19 during the period where the Omicron variant was dominant in New York
34 compared to non-infected MM patients. Antibody concentrations measured in artificial
35 units per mL (AU/mL) and are depicted on a log-10 scale. The horizontal dotted line
36 indicates the lower limit of detection (5 AU/mL). **(J)** Neutralizing antibody ID50 to Omicron
37 SARS-CoV-2 strain for MM subject groups and HD. The bold horizontal line indicates the
38 median for each group. **(K)** Quantification of MM patients and HD that achieve
39 neutralization to Omicron strain >1 week post dose 2 and >1 week post dose 3. **(L)**
40 Spearman's rank correlation between anti-S IgG antibody levels and WA1, wildtype
41 neutralizing ID50. **(M)** Spearman's rank correlation between anti-S IgG antibody levels
42 and Omicron variant neutralizing ID50. The lower and upper hinges of the boxplot
43 correspond to the first and third quartiles (the 25th and 75th percentiles) with a bold
44 horizontal line indicating the median. Vertical whiskers are extended up to 1.5 times the
45 interquartile range (IQR). P-values represent comparison using the non-parametric

- 46 Mann-Whitney U test. P-values for contingency outcomes represent comparison using
- 47 Fisher's exact test; (ns) $p > 0.05$, (*) $p < 0.05$, (**) $p < 0.01$, (***) $p < 0.001$, (****) $p < 0.0001$.

48 **Supplemental Table S1. Clinical characteristics of patients with multiple myeloma and**
 49 **healthy donor controls.**

VARIABLE	MM COHORT (N = 476)		HD (N=45)	
Age (y)	67	[38-96]	58	[49-71]
Male gender	56.7%	(270)	24%	(11)
Vaccine Type Initial Dose				
Pfizer-BioNTech	70.6%	(336)	73%	(33)
Moderna	29.4%	(140)	27%	(12)
Received ≥2 documented doses	99.2%	(472)	100%	(45)
Received ≥3 documented doses	72.5%	(345)	100%	(45)
Timing of dose 3 after dose 2 (d)	207	[41-360]	280	[208-361]
Heterologous vaccination regimen	5.8%	(20/345)	4%	(2)
Had documented COVID-19	26.1%	(124)	44%	(20)
Disease Isotype				
IgG	60.1%	(286)		
IgA	20.2%	(96)		
LC	18.9%	(90)		
Other	0.8%	(4)		
SMM	8.4%	(40)		
Time since diagnosis (mo)	64.9	[0-254]		
> 3 previous lines of treatment	28.2%	(134)		
> 5 previous lines of treatment	16.2%	(77)		
Disease response status				
CR or sCR	40.5%	(193)		
VGPR	17.6%	(84)		
PR or MR	8.2%	(39)		
SD or PD	19.1%	(91)		
Unable to assess	14.3%	(68)		
Treatment regimen at initial vaccination contains:				
Immunomodulatory drug	46.2%	(220)		
Proteasome inhibitor	6.1%	(129)		
Anti-CD38 mAb	40.3%	(192)		
Anti-SLAMF7 mAb	5.0%	(24)		
BCMA-targeted therapy	10.7%	(51)		
BCMA-targeted bispecific	3.4%	(16)		
CAR T cell therapy	6.1%	(29)		
Other BCMA-targeted therapy	1.3%	(6)		
Other bispecific (non-BCMA)	4.2%	(20)		
Other therapy (incl. venetoclax, selinexor, alkylators)	8.2%	(39)		
Previous ASCT	49.8%	(237)		
ASCT < 12 mo before dose 1	6.3%	(30)		
No active treatment	19.3%	(92)		
Note: values are presented as percentage (n) or median [range]. Disease response status and treatment regimen were registered at the date of administration of the first dose of mRNA vaccine.				
Abbreviations: y, years; mo, months; COVID-19, coronavirus disease 2019; Ig, immunoglobulin; MM, multiple myeloma; SMM, smoldering multiple myeloma; HD, healthy donor; CR, complete response; sCR, stringent complete response; VGPR, very good partial response; PR, partial response; MR, minimal response; SD, stable disease; PD; progressive disease; ASCT, autologous stem cell transplant; mAb, monoclonal antibody; BCMA, B-cell maturation antigen; CAR, chimeric antigen receptor				

51 **Supplemental Materials and Methods:**

52

53 **Study information and patient selection.** Multiple myeloma (MM) patients: The serology study
54 cohort consisted of 476 patients with and without previously documented COVID-19 pooled from
55 two different non-interventional Institutional Review Board (IRB) approved study protocols at The
56 Icahn School of Medicine at Mount Sinai. A total of 279 MM patients were enrolled after obtaining
57 written informed consent for the MARS study, an ongoing longitudinal study at our institution (IRB-
58 16-00791). Patients had blood and saliva taken for analysis at multiple time points before or after
59 administration of the SARS-CoV-2 mRNA vaccine. All specimens were coded prior to processing
60 and antibody testing for all serum specimen was performed in a blinded manner. All participants
61 with, at least, one post vaccine antibody data point available at the time of writing this report were
62 included in the analysis. The remaining 197 MM patients were identified under a retrospective
63 study (IRB: GCO#: 11-1433) by conducting a chart review for patients at our MM clinic who had
64 SARS-CoV-2 spike IgG results at various time points around SARS-CoV-2 mRNA vaccine
65 administration. Chart review was conducted to retrieve patient clinical characteristics.

66

67 All 31 MM patients used in cellular and neutralization assays consented to enrollment in the MARS
68 clinical trial IRB: 16-00791. The study was approved by the Program for Protection of Human
69 Subject an Institutional Review Board approved research study. Peripheral blood was collected
70 in heparin green tops (Cat#362761), BD Vacutainer CPT (Cat#367985) and BD SST™ Serum
71 Separation Tubes (Cat#0268396) via venipuncture according to trial schedule. Peripheral blood
72 mononuclear cells (PBMC) were Ficoll density separated and cryopreserved by the MARS
73 processing team. Cryopreserved PBMC samples were used to Flow Cytometry analysis. Sera
74 isolated from blood was used to SARS-CoV-2 antibody ELISA and neutralizing assay.

75

76 Healthy donors (HD) group: 13 participants of the PARIS (Protection Associated with Rapid
77 Immunity to SARS-CoV-2) study were selected as controls to best match the demographics of
78 the 31 MM patient population. The PARIS cohort follows health care workers longitudinally to
79 assess the durability and effectiveness of SARS-CoV-2 immune responses. The study was
80 reviewed and approved by the Mount Sinai Hospital Institutional Review Board (IRB-20-03374).
81 All participants provided written informed consent prior to collection of data and specimen.

82

83 Both studies were carried out in compliance with the Declaration of Helsinki and International
84 Conference on Harmonization Guidelines for Good Clinical Practice. Chart review was conducted
85 to retrieve patient clinical characteristics. Anti-SARS-CoV-2 antibody testing was performed using
86 an anti-IgG assay developed at Mount Sinai Health System Department of Pathology in
87 collaboration with the Icahn School of Medicine at Mount Sinai Department of Microbiology under
88 a Food and Drug Administration (FDA) Emergency Use Authorization.

89

90 **SARS-CoV-2 antibody ELISA.** Antibodies to SARS-CoV-2 spike were detected using an
91 established quantitative two-step ELISA termed Mount Sinai Antibody test described in detail in
92 the referenced manuscripts.(Stadlbauer et al., 2020; Stadlbauer et al., 2021) The assay shows a
93 performance of 100% specificity and 95% sensitivity in in-house evaluation.

94

95 **Flow cytometry assay to detect SARS-CoV-2 spike-reactive B cells.** SARS-CoV-2 spike-
96 reactive B cells were detected with a in house antibody panel (Panel A) developed to
97 simultaneously detect spike-reactive B cells along with immunophenotyping of myeloid and
98 lymphoid cells in peripheral blood. Recombinant spike protein used is known as OptSpike1
99 which is cloned into the mammalian expression vector pCAGGS and includes the majority of the
100 ectodomain (OptSpike1: AAs 1–1208). Spike protein purification and production described in
101 detail in the referenced manuscript. (Herrera et al., 2021) Strategy to detect spike-reactive B

102 cells have been described in our previous report (Aleman et al., 2021). Thawed PBMC were
103 initially stained with Live/Dead Fixable Blue Dead Cell Stain Kit (L23105, Thermofisher
104 Scientific) for 15 minutes at room temperature. Viability dye stained PBMC were further stained
105 with Panel A in multiple staining steps at different temperatures. PBMC were stained at room
106 temperature for 15 minutes with a cocktail of 14 antibodies, washed and further stained with
107 spike protein for 30 mins on ice. Post spike protein staining PBMC were washed and stained on
108 ice for 30 minutes with equal amounts of anti-Strep II-FITC and anti-Strep II-Biotin antibodies
109 (A01736, A01737, GeneScript) at a dilution of 1:150. Washed PBMC were further stained with a
110 cocktail of remaining antibodies in Panel A including APC labeled Streptavidin (BioLegend) for
111 30 minutes on ice. Antibodies in Panel A stained at room temperature include CCR6-BUV496
112 (clone 11Ag), CD45RA-BUV563 (clone HI100), CD28-BUV737 (clone 28.2) (all from BD
113 Biosciences), TCR gamma-delta-PerCP-eFluor710 (clone B1.1, Thermofisher), CCR7-BV421
114 (clone G043H7), CXCR3-BV510 (clone G025H7), CD27-BV570 (clone O323), CXCR5-BV605
115 (clone J25D4), CRTH2-BV711(clone BM16),PD-1-BV750 (clone EH12.1H7),CD25-PE (clone M-
116 A251), CD66b-PE-Dazzle 594 (clone QA17A51), CCR4-PE-FIRE 810 (clone L291H4), CD11c-
117 Alexa700 (clone Bu15) (all from BioLegend). Antibodies in Panel A stained on ice include CD4-
118 BUV395 (clone SK3), CD56-BUV615 (clone NCAM16.2), HLA-DR-BUV661 (clone G46-6), CD3-
119 BUV805 (clone UCHT1), CD20-BV480 (clone 2H7) (all from BD Biosciences), CD1c-
120 SuperBright 436 (clone L161), CD123-eFluor450 (clone 6H6), CD8-NFB555 (clone OKT8),
121 CD19-NFB610-70S (clone HIB19), CD14-NFB660-40S (clone MEM-15), CD127-PE-Cy5.5
122 (clone eBioRDR5), CD16-NFR685 (clone 3G8) (all from Thermofisher), IgM-BV650 (clone
123 MHM-88), IgD-BV785(IA6-2), CD11b-PerCP (clone M1/70), CD57-PerCP-Cy5.5 (clone HNK-1),
124 CD24-PE-Cy5 (clone ML5), IgG Fc-PE-Cy7 (clone M1310G05) CD38-APC-FIRE810 (clone
125 HIT2) (all from BioLegend), IgA-APC-VIO770 (clone IS11-8E10, Miltenyi Biotec) Anti-Strep II-
126 FITC, Anti-Strep II-Biotin. Each antibody was used at a dilution of 1:25. All antibody cocktail
127 preparations included True-Stain Monocyte buffer (Biolegend), CellBlox Monocyte and

128 Macrophage blocking buffer (Thermofisher) and Super Bright Complete Staining buffer
129 (Thermofisher) at a dilution of 1:20 to avoid nonspecific dye-dye and dyes to cell interaction.
130 Cells were acquired on Cytex Aurora Flow Cytometer (Cytex Biosciences). Flow data was
131 compensated on Cytex Aurora acquisition software SpectroFlo and compensated .fcs files were
132 exported to Flowjo software (BD Biosciences) for analysis. Supervised hierarchal gating was
133 employed to delineate major cell types and identify spike-reactive B cells in PBMC. Total cells
134 were initially gated to remove dead cells, doublets and CD66b+ cells. From the live CD66b
135 negative cell gate monocytes were identified based on expression of markers CD16 and CD14
136 (CD16hi/-CD14-/+). Monocyte-negative cells were sequentially gated for markers CD1c, CD123
137 and CD19 (CD1c vs CD123 followed by CD1c vs CD19 on CD123- cells) to identify
138 plasmacytoid dendritic cells (pDC, CD123+CD1c-) and conventional dendritic cells (cDC,
139 CD123-CD19-CD1c+). pDC and cDC negative cell fraction was gated for CD3 and CD38 to
140 identify total T cells (CD3+CD38+/-). Subsequently B cells were identified from the CD3
141 negative gate as cells expressing HLADR and CD19 (CD19+HLADR+/-). As described in our
142 previous report (Aleman *et al.*, 2021), B cells showing fluorescent signals for both Strep-II-FITC
143 and Strep-II-Biotin-Streptavidin-APC were classified as spike-reactive B cells. Finally, B cell-
144 negative cells were plotted as CD56 vs CD16 to identify NK cells (CD56hiCD16- and
145 CD56dimCD16+ NK cells). PBMC from healthy donors prior to any SARS-CoV-2 vaccination or
146 SARS-CoV-2 exposure were stimulated similarly and were used as a control group.

147

148 **Intracellular cytokine staining flow cytometry (ICS-Flow) T cell assay.** T cell assays were
149 carried out in RPMI supplemented with 10% Human Ab serum (R&D Systems), 1x glutamax
150 (Lonza) 1x Penicillin-Streptomycin. PBMC were stimulated for 6 hours with a pool of spike
151 peptides (15-mer sequences with 11 amino acids overlap spanning the entire spike protein,
152 Miltenyi Biotec) at concentrations recommended by the manufacturer or with water as control
153 along with co-stimulators for CD28 and CD49d (i.e., anti-CD28 clone CD28.1 and anti-CD49d

154 clone 9F109, both from Biolegend). Culture conditions also included antibodies to detect CD4
155 activation marker CD154 and CD8 degranulation marker CD107 (CD154-PE, clone 24-31 and
156 CD107a-FITC, clone H4A3 both from BioLegend) and Monensin (BioLegend). Stimulations with
157 Staphylococcal enterotoxin B (SEB) were used as positive control. Post stimulation cells were
158 washed and stained with Live/Dead Fixable Blue Dead Cell Stain Kit for 15 minutes at room
159 temperature followed by surface staining with a cocktail of antibodies comprising of CD3- BUV805
160 (clone UCHT1), CD4-BUV395 (clone SK3), CD8-BUV496 (clone RPA-T8), CD45RA-BUV563
161 (clone HI100), PD-1-BUV615 (clone EH12.1), HLA-DR-BUV661 (clone G46-6) (all from BD
162 Biosciences,) CCR7-BV510 (clone G043H7), CD27-BV570 (clone O323), CD69-BV605 (clone
163 FN50), CD200-BV711 (clone OX-104), CXCR5-BV785 (clone J252D4), ICOS-PE-Dazzle594
164 (clone QA17A51), OX40-PE-Cy5 (clone Ber-ACT35) 4-1bb-APC-Fire750 (clone 4B4-1) (all from
165 BioLegend) and CD19-NFB610-70S (clone HIB19). After surface marker staining cells were fixed
166 with 4% paraformaldehyde (PFA) and permeabilized with BD perm buffer (BD Biosciences) and
167 stained with a cocktail of antibodies to cytokines IL-4 (IL-4-BUV737, clone MP4-25D2), IL-17 (IL-
168 17-BV650, clone N49-653) (both from BD Biosciences), IFN-g (IFN-g-BV421, clone B27), TNF-
169 α (TNF- α -PE-Cy7, clone MaB11), IL-2 (IL-2-APC, clone MQ1-17H12) and GM-CSF (GM-CSF-
170 PerCP-Cy5.5) (all from BioLegend). The cells were acquired on Cytex Aurora Flow Cytometer.
171 Flow data was compensated on Cytex Aurora acquisition software SpectroFlo and compensated
172 .fcs files were exported to Flowjo software (BD Biosciences) for analysis. Data was gated to
173 exclude dead cells and doublets and then further gated on forward scatter (FSC-A) vs side scatter
174 (SSC-A) plot to identify lymphocytes. CD3 vs CD19 plots on lymphocytes were used to identify
175 total T cells (CD3+). Total T cells were further gated to identify CD4+ and CD8+ T cells. Activated
176 CD4+ T cell population were identified by the expression of activation markers CD154 or CD69
177 as described in our previous report (Aleman *et al.*, 2021). Total cytokine responses in CD4+ T
178 cells were quantified by performing Boolean gating for each cytokine on activated CD4+ T cells.
179 Events from each cytokine combination were pooled and divided by total CD4 T cells events to

180 calculate the frequency of total cytokine positive CD4+ T cells. Finally, SARS-CoV-2 spike-
181 specific CD4+ T cell response was calculated by subtracting water control total cytokine
182 frequencies from SARS-CoV-2 spike peptide-stimulated conditions. Negative values were
183 designated as zero. PBMC from healthy donors prior to any SARS-CoV-2 vaccination or SARS-
184 CoV-2 exposure were stimulated similarly and were used as a control group.

185

186 **Cells and SARS-CoV-2 isolates.** Vero-E6-TMPRSS2 cells were cultured in Dulbecco's modified
187 Eagles medium (DMEM; Corning) supplemented 10% heat-inactivated fetal bovine serum (FBS;
188 GeminiBio) and 1% minimum essential medium (MEM) amino acids solution (Gibco), 100 U/ml
189 penicillin, 100 µg/ml streptomycin (Gibco), 100 µg/ml normocin (InvivoGen, #ant-nr), and 3 µg/ml
190 puromycin (InvivoGen). The authentic SARS-CoV-2 virus (USA-WA1/2020;
191 GenBank: [MT020880](#)) was obtained from BEI resources. (BEI resources, NR-52281). The
192 B.1.1.529 isolate USA/NY-MSHSPSP-PV44488/2021 (BA.1, EPI_ISL_7908059) was previously
193 described.(Carreno et al., 2022) Viruses were grown and tittered on Vero-E6-TMPRSS2 cells.

194

195 **SARS-CoV-2 multi-cycle microneutralization assay.** Serum samples from study participants
196 were used to determine the neutralization of wild type (WA1), and B.1.1.529 (Omicron) SARS-
197 CoV-2 isolates. All procedures were performed in a biosafety level 3 (BSL-3) facility at the Icahn
198 School of Medicine at Mount Sinai following standard safety guidelines. The day before infection,
199 Vero-E6-TMPRSS2 cells were seeded in 96-well high binding cell culture plates (Costar,
200 #07620009) at a density of 20,000 cells/well in complete Dulbecco's modified Eagle medium
201 (cDMEM) one day prior to the infection. After heat inactivation of sera (56°C for 1 hour), serum
202 samples were serially diluted (3-fold) in minimum essential media (MEM; Gibco, #11430-030)
203 supplemented with 2 mM L-glutamine (Gibco, #25030081), 0.1% sodium bicarbonate (w/v,
204 HyClone), 10 mM 4-(2-hydroxyethyl)-1-piperazineethanesulfonic acid (HEPES), 100 /ml penicillin,
205 100 µg/ml streptomycin (Gibco) and 0.2% bovine serum albumin (BSA, MP Biomedicals, Cat#.

206 810063) starting at 1:10. Remdesivir (Medkoo Bioscience Inc.) was included to monitor assay
207 variation. Serially diluted sera were incubated with 10,000 TCID₅₀ of WT USA-WA1/2020 SARS-
208 CoV-2, or USA/NY-MSHSPSP-PV44488/2021 (B.1.1.529, Omicron) for one hour at RT, followed
209 by the transfer of 120µl of the virus-sera mix to Vero-E6-TMPRSS2 plates. Infection proceeded
210 for one hour at 37°C and inoculum was removed. 100 µl/well of the corresponding antibody
211 dilutions plus 100µl/well of infection media supplemented with 2% fetal bovine serum (FBS; Gibco,
212 #10082-147) were added to the cells. Plates were incubated for 48h at 37°C followed by fixation
213 overnight at 4°C in 200 µl/well of a 10% formaldehyde solution. For staining of the nucleoprotein,
214 formaldehyde solution was removed, and cells were washed with PBS (pH 7.4) (Gibco) and
215 permeabilized by adding 150 µl/well of PBS, 0.1% Triton X-100 (Fisher Bioreagents) for 15 min at
216 RT. Permeabilization solution was removed, plates were washed with 200 µl/well of PBS (Gibco)
217 twice and blocked with PBS, 3% BSA for 1 hour at RT. During this time the primary antibody was
218 biotinylated according to manufacturer protocol (Thermo Scientific EZ-Link NHS-PEG4-Biotin).
219 Blocking solution was removed and 100 µl/well of biotinylated mAb 1C7C7, a mouse anti-SARS
220 nucleoprotein monoclonal antibody generated at the Center for Therapeutic Antibody
221 Development at The Icahn School of Medicine at Mount Sinai ISMMS (Millipore Sigma) at a
222 concentration of 1µg/ml in PBS, 1% BSA was added for 1 hour at RT. Cells were washed with
223 200 µl/well of PBS twice and 100 µl/well of HRP-conjugated streptavidin (Thermo Fisher
224 Scientific) diluted in PBS, 1% BSA were added at a 1:2,000 dilution for 1 hour at RT. Cells were
225 washed twice with PBS, and 100 µl/well of o-phenylenediamine dihydrochloride (Sigmafast OPD;
226 Sigma-Aldrich) were added for 10 min at RT, followed by addition of 50 µl/well of a 3 M HCl
227 solution (Thermo Fisher Scientific). Optical density (OD) was measured (490 nm) using a
228 microplate reader (Synergy H1; Biotek). Analysis was performed using Prism 9 software
229 (GraphPad). After subtraction of background and calculation of the percentage of neutralization
230 with respect to the “virus only” control, a nonlinear regression curve fit analysis was performed to
231 calculate the 50% inhibitory dilution (ID₅₀), with top and bottom constraints set to 100% and 0%

232 respectively. All samples were analyzed in a blinded manner. Viral isolates composition and
233 methods are described in more detail in our previous publication (Carreno *et al.*, 2022).

234

235 **Statistical Analysis.** The Mann-Whitney U test was used to determine significance for all
236 continuous variables that were non-parametrically distributed. Fisher's exact test was used to
237 determine significance in outcome measures. A two-sided alpha < 0.05 was considered
238 statistically significant. Differences between continuous variables and contingency variables were
239 done using R (v4.0.2). All statistical tests were run with R (v4.0.2).

240

241 **Supplemental References:**

242 Aleman, A., Upadhyaya, B., Tuballes, K., Kappes, K., Gleason, C.R., Beach, K., Agte, S.,
243 Srivastava, K., Group, P.V.S.S., Van Oekelen, O., et al. (2021). Variable cellular
244 responses to SARS-CoV-2 in fully vaccinated patients with multiple myeloma. *Cancer*
245 *Cell* 39, 1442-1444.

246 Carreno, J.M., Alshammary, H., Tcheou, J., Singh, G., Raskin, A.J., Kawabata, H.,
247 Sominsky, L.A., Clark, J.J., Adelsberg, D.C., Bielak, D.A., et al. (2022). Activity of
248 convalescent and vaccine serum against SARS-CoV-2 Omicron. *Nature* 602, 682-688.

249 Herrera, N.G., Morano, N.C., Celikgil, A., Georgiev, G.I., Malonis, R.J., Lee, J.H., Tong,
250 K., Vergnolle, O., Massimi, A.B., Yen, L.Y., et al. (2021). Characterization of the SARS-
251 CoV-2 S Protein: Biophysical, Biochemical, Structural, and Antigenic Analysis. *ACS*
252 *Omega* 6, 85-102.

253 Stadlbauer, D., Amanat, F., Chromikova, V., Jiang, K., Strohmeier, S., Arunkumar, G.A.,
254 Tan, J., Bhavsar, D., Capuano, C., Kirkpatrick, E., et al. (2020). SARS-CoV-2

255 Seroconversion in Humans: A Detailed Protocol for a Serological Assay, Antigen
256 Production, and Test Setup. *Curr Protoc Microbiol* 57, e100.

257 Stadlbauer, D., Tan, J., Jiang, K., Hernandez, M.M., Fabre, S., Amanat, F., Teo, C.,
258 Arunkumar, G.A., McMahon, M., Capuano, C., et al. (2021). Repeated cross-sectional
259 sero-monitoring of SARS-CoV-2 in New York City. *Nature* 590, 146-150.

260

261